BEM-based Finite Element Tearing and Interconnecting Methods

Clemens Hofreither

Institute of Computational Mathematics, Johannes Kepler University
Altenberger Str. 69, 4040 Linz, Austria

Ulrich Langer

Institute of Computational Mathematics, Johannes Kepler University
and
Johann Radon Institute for Computational and Applied Mathematics
(RICAM), Austrian Academy of Sciences,
Altenberger Str. 69, 4040 Linz, Austria

Clemens Pechstein

Institute of Computational Mathematics, Johannes Kepler University
Altenberger Str. 69, 4040 Linz, Austria

Technical Reports before 1998:

1995

95-1	Hedwig Brandstetter	
	Was ist neu in Fortran 90?	March 1995
95-2	G. Haase, B. Heise, M. Kuhn, U. Langer	
	Adaptive Domain Decomposition Methods for Finite and Boundary Element Equations.	August 1995
95-3	Joachim Schöberl	
	An Automatic Mesh Generator Using Geometric Rules for Two and Three Space Dimensions.	August 1995

1996

96-1	Ferdinand Kickinger	
	Automatic Mesh Generation for 3D Objects.	February 1996
96-2	Mario Goppold, Gundolf Haase, Bodo Heise und Michael Kuhn	
	Preprocessing in BE/FE Domain Decomposition Methods.	February 1996
96-3	Bodo Heise	
	A Mixed Variational Formulation for 3D Magnetostatics and its Finite Element Discretisation.	February 1996
96-4	Bodo Heise und Michael Jung	
	Robust Parallel Newton-Multilevel Methods.	February 1996
96-5	Ferdinand Kickinger	
	Algebraic Multigrid for Discrete Elliptic Second Order Problems.	February 1996
96-6	Bodo Heise	
	A Mixed Variational Formulation for 3D Magnetostatics and its Finite Element Discretisation.	May 1996
96-7	Michael Kuhn	
	Benchmarking for Boundary Element Methods.	June 1996

1997

97-1	Bodo Heise, Michael Kuhn and Ulrich Langer	
	A Mixed Variational Formulation for 3D Magnetostatics in the Space $H(rot) \cap H(div)$	February 1997
97-2	Joachim Schöberl	
	Robust Multigrid Preconditioning for Parameter Dependent Problems I: The Stokes-type Case.	June 1997
97-3	Ferdinand Kickinger, Sergei V. Nepomnyaschikh, Ralf Pfau, Joachim Schöberl	
	Numerical Estimates of Inequalities in $H^{\frac{1}{2}}$.	August 1997
97-4	Joachim Schöberl	
	Programmbeschreibung NAOMI 2D und Algebraic Multigrid.	September 1997

BEM-BASED FINITE ELEMENT TEARING AND INTERCONNECTING METHODS

CLEMENS HOFREITHER[1†], ULRICH LANGER[2†‡], AND CLEMENS PECHSTEIN[3†]

ABSTRACT. We present efficient domain decomposition solvers for a class of non-standard finite element methods (FEM). These methods utilize PDE-harmonic trial functions in every element of a polyhedral mesh, and use boundary element techniques locally in order to assemble the finite element stiffness matrices. For these reasons, the terms BEM-based FEM or Trefftz-FEM are sometimes used in connection with this method. In the present paper, we show that finite element tearing and interconnecting (FETI) methods can be used to solve the resulting linear systems in a quasi-optimal, robust, and parallel manner. Spectral equivalences between certain approximations of element-local Steklov-Poincaré operators play a central role in transferring the known convergence results for FETI to this new method. The theoretical results are supplemented by numerical tests confirming the theoretical predictions.

1. INTRODUCTION

This paper is devoted to the construction and analysis of fast and robust solution methods for a new class of non-standard finite element schemes which was introduced by Copeland, Langer and Pusch [2] and developed in a series of publications in recent years [1, 10, 8, 31, 12, 26, 32, 9].

The characteristic features of this new method are the following: (1) instead of homogeneous simplicial or hexahedral meshes, spatial discretizations which consist of arbitrary, even non-convex, polygons or polyhedra are admitted; (2) trial functions are constructed as local solutions of the partial differential solution with simple, usually piecewise linear boundary data on each element; (3) Green's formula then permits the reduction of the variational equation to the element boundaries, leading so a so-called skeletal variational formulation; (4) techniques based on boundary element methods (BEM) are used in order to approximate the Dirichlet-to-Neumann maps which are associated to the element-local problems. On the other hand, the

method shares many characteristic features with the finite element method: it is a Galerkin method which employs trial functions with local support and which preserves symmetry and coercivity of the underlying partial differential operator in the discretized system. Indeed, it can be viewed as a finite element method where the element stiffness matrices are computed using boundary element techniques. Therefore, the method has been dubbed "BEM-based FEM" in the literature.

Previous publications on this method have investigated a priori error estimates [10, 8], a posteriori error estimators and adaptive refinement [31], generalizations to higher-order trial functions [26], and applications to Helmholtz and Maxwell equations [1, 2] as well as convection-diffusion problems [11]. The main results have been collected in two PhD theses [32, 9].

In the present work, we turn our attention to the efficient solution of the linear systems arising from the BEM-based FEM discretization of second-order scalar elliptic partial differential equations (PDEs) such as the diffusion equation in two and three spatial dimensions. While early experiments with algebraic multigrid solvers have shown promising results [2], herein we focus on a domain decomposition approach based on the finite element tearing and interconnecting (FETI) method. The FETI method was introduced by Farhat and Roux in [7] and has been generalized and analyzed by numerous researchers, see, e.g., the monographs [30] and [20] for the corresponding references. Our main goal in this article is to demonstrate that the FETI method as well as commonly used preconditioners can be adapted with only minor modifications to the setting of the BEM-based FEM. Furthermore, by proving certain spectral equivalences for the Schur complements arising in this new FETI-like scheme, we are able to transfer known condition number estimates from the FETI literature to the new BEM-based FETI solver.

We mention that the boundary element tearing and interconnecting (BETI) method, introduced by Langer and Steinbach [14] as the boundary element counterpart of the FETI method, bears a certain similarity to the scheme we will derive here. Indeed, the BETI method corresponds to the case where every subdomain is a single BEM domain, while in the new FETI-like scheme for the BEM-based FEM, subdomains are typically agglomerates of several BEM domains coupled together. The convergence analysis of the BETI method is heavily based on spectral equivalences between FEM- and BEM-approximated Steklov-Poincaré operators. As mentioned above, similar techniques are used for the convergence analysis of the new scheme considered in this paper.

The remainder of this paper is structured as follows. In Section 2, we derive the skeletal variational formulation which serves as the starting point for discretization in the BEM-based FEM. In Section 3, we introduce BEM-based approximations of Steklov-Poincaré operators. In Section 4, we introduce discretized spaces and obtain a discrete scheme. In Section 5, we derive our BEM-based FETI solution method for these discrete linear systems. Then we establish the convergence analysis for this domain decomposition method in Section 6. In Section 7, we present and discuss some results of our numerical experiments. Section 8 concludes the paper with some final remarks.

2. Derivation of a skeletal variational formulation

We give a brief derivation of the BEM-based FEM and refer to [10, 9] for further details.

Let $\Omega \subset \mathbb{R}^d$, $d = 2$ or 3, be a bounded Lipschitz domain. We consider the mixed boundary value problem for the potential equation,

$$\left. \begin{aligned} -\operatorname{div}(\alpha \nabla u) &= f && \text{in } \Omega, \\ u &= g_D && \text{on } \Gamma_D, \\ \alpha \frac{\partial u}{\partial n} &= g_N && \text{on } \Gamma_N \end{aligned} \right\} \tag{2.1}$$

where $\alpha = \alpha(x) \geq \alpha_0 > 0$ is a given bounded, uniformly positive diffusion coefficient, f is a given forcing term, $\Gamma_D \subseteq \partial\Omega$ is the Dirichlet boundary with prescribed values g_D and has positive surface measure, and $\Gamma_N = \partial\Omega \setminus \overline{\Gamma}_D$ is the Neumann boundary with prescribed conormal derivative g_N.

The standard variational formulation of (2.1) is given by

$$\int_\Omega \alpha \nabla u \cdot \nabla v \, dx = \int_\Omega f v \, dx + \int_{\Gamma_N} g_N v \, ds \qquad \forall v \in H_D^1(\Omega), \tag{2.2}$$

where $H_D^1(\Omega) = \{v \in H^1(\Omega) : v|_{\Gamma_D} = 0\}$ is the space of H^1-functions which vanish on the Dirichlet boundary. Here, u is sought in the manifold of H^1-functions which match g_D on Γ_D.

Consider a decomposition $\mathcal{T}$ of the domain Ω into polytopal elements $T \in \mathcal{T}$. In contrast to a standard FEM method, we do not restrict ourselves to homogeneous element topologies, but allow the mesh to consist of a mixture of rather general polygons (in 2D) or polyhedra (in 3D). We assume that the coefficient function α is piecewise constant with respect to $\mathcal{T}$, i.e., $\alpha(x) = \alpha_T \ \forall x \in T$, $\forall T \in \mathcal{T}$. The mesh size will be denoted by $h = \max_{T \in \mathcal{T}} \operatorname{diam}(T)$.

We now formulate a homogeneous local problem on every element T. Namely, given $g_T \in H^{1/2}(\partial T)$, find $u_T \in H^1(T)$ with $u_T|_{\partial T} = g_T$ such that

$$\int_T \alpha_T \nabla u_T \cdot \nabla v_T \, dx = 0 \qquad \forall v_T \in H_0^1(T).$$

This local problem is uniquely solvable, and we denote the mapping $g_T \mapsto u_T$ by the local harmonic extension operator $\mathcal{H}_T : H^{1/2}(\partial T) \to H^1(T)$. It is elementary that $\mathcal{H}_T$ minimizes the H^1-energy in the sense that

$$|\mathcal{H}_T g_T|_{H^1(T)} = \inf_{\substack{w_T \in H^1(T) \\ w_T|_{\partial T} = g_T}} |w_T|_{H^1(T)}. \tag{2.3}$$

We now define the local Steklov-Poincaré operator $S_T : H^{1/2}(\partial T) \to H^{-1/2}(\partial T)$ which maps $u \in H^{1/2}(\partial T)$ to the functional

$$\langle S_T u, v \rangle := \int_T \alpha_T \nabla(\mathcal{H}_T u) \cdot \nabla(\mathcal{H}_T v) \, dx \qquad \forall v \in H^{1/2}(\partial T).$$

In case of sufficient smoothness, Green's formula yields $S_T u = \alpha_T \partial_n(\mathcal{H}_T u)$, i.e., $S_T u$ is the conormal derivative of the harmonic extension. Therefore,

S_T is also called the *Dirichlet-to-Neumann map*. From the definition, it immediately follows that

$$\langle S_T v, v \rangle = \alpha_T \, |\mathcal{H}_T v|^2_{H^1(T)}. \tag{2.4}$$

If we introduce the *skeleton* $\Gamma_S := \bigcup_{T \in \mathcal{T}} \partial T$ as the union of all element boundaries and denote by $H^{1/2}(\Gamma_S)$ the trace space of $H^1(\Omega)$-functions onto the skeleton (in the sense of the usual Sobolev trace operator), we can formulate the skeletal variational problem: find $u \in H^{1/2}(\Gamma_S)$ with $u|_{\Gamma_D} = g_D$ such that

$$a(u, v) = \langle F, v \rangle \qquad \forall v \in \mathcal{W}_D, \tag{2.5}$$

where

$$a(u, v) := \sum_{T \in \mathcal{T}} \langle S_T u|_{\partial T}, \, v|_{\partial T} \rangle,$$

$$\langle F, v \rangle := \sum_{T \in \mathcal{T}} \left[\int_T f \mathcal{H}_T(v|_{\partial T}) \, dx + \int_{\partial T \cap \Gamma_N} g_N v \, ds \right],$$

$$\mathcal{W}_D := \{ v \in H^{1/2}(\Gamma_S) : v|_{\Gamma_D} = 0 \}.$$

It can be shown that this skeletal formulation is equivalent to the standard variational formulation (2.2) in the sense that the solution of the former is the skeletal trace of the solution of the latter [10, 9].

3. Approximation of the Steklov-Poincaré operator

The Steklov-Poincaré operator S_T appearing in the variational formulation (2.5) does not admit an exact evaluation in general. In the following, we give a rather standard computable approximation in terms of boundary integral operators.

A fundamental solution for the Laplace operator in $\mathbb{R}^d$ is given by

$$G(x, y) := \begin{cases} -\frac{1}{2\pi} \log |x - y| & \text{if } d = 2, \\ \frac{1}{4\pi} |x - y|^{-1} & \text{if } d = 3, \end{cases}$$

see, e.g., [27, 29]. Based on this, we define on the boundary of every element $T \in \mathcal{T}$ the local boundary integral operators (cf. [27, 29])

$$V_T : H^{-1/2}(\partial T) \to H^{1/2}(\partial T), \quad K_T : H^{1/2}(\partial T) \to H^{1/2}(\partial T),$$
$$K'_T : H^{-1/2}(\partial T) \to H^{-1/2}(\partial T), \quad D_T : H^{1/2}(\partial T) \to H^{-1/2}(\partial T),$$

called, in turn, the *single layer potential*, *double layer potential*, *adjoint double layer potential*, and *hypersingular* operators. For sufficiently smooth functions, they admit the integral representations

$$(V_T v)(y) = \int_{\partial T} G(x, y) v(x) \, ds_x,$$

$$(K_T u)(y) = \int_{\partial T} \Big(\frac{\partial}{\partial n_{T,x}} G(x, y)\Big) u(x) \, ds_x,$$

$$(K_T' v)(y) = \int_{\partial T} \frac{\partial}{\partial n_{T,y}} G(x, y) v(x) \, ds_x,$$

$$(D_T u)(y) = -\frac{\partial}{\partial n_{T,y}} \int_{\partial T} \Big(\frac{\partial}{\partial n_{T,x}} G(x, y)\Big) \big(u(x) - u(y)\big) \, ds_x.$$

Let us mention that V_T and D_T are self-adjoint whereas K_T and K_T' are adjoint to each other. For $d = 2$, we make the additional technical assumption $\mathrm{diam}(T) < 1$ for all $T \in \mathcal{T}$ throughout, to ensure that V_T is invertible.

It can be shown [27, 29] that the Steklov-Poincaré operator S_T can be expressed in terms of the boundary integral operators via the two expressions

$$S_T = \alpha_T(V_T^{-1}(\tfrac{1}{2}I + K_T)) = \alpha_T(D_T + (\tfrac{1}{2}I + K_T')V_T^{-1}(\tfrac{1}{2}I + K_T)). \quad (3.1)$$

Both of these representations contain the inverse of the single layer potential operator, which is not readily computable. We therefore construct a computable approximation as described in the following.

We assume that each element boundary ∂T has a shape-regular mesh $\mathcal{F}_T$ which consists of line segments in $\mathbb{R}^2$ and of triangles in $\mathbb{R}^3$. We further assume that these local meshes are matching across elements in the sense that for any two elements T_1 and T_2 having a common interface $\Gamma_{12} = \partial T_1 \cap \partial T_2$ with positive measure, any triangle $\tau \in \mathcal{F}_{T_1}$ with $\tau \cap \Gamma_{12} \neq \emptyset$ should also belong to $\mathcal{F}_{T_2}$. In other words, element interfaces must be triangulated identically in both elements.

On the boundary mesh $\mathcal{F}_T$, we construct a space $\mathcal{Z}_T^h$ of piecewise constant (per boundary element $\tau \in \mathcal{F}_T$) functions and define, given $u \in H^{1/2}(\partial T)$, the discrete variable $w_T^h \in \mathcal{Z}_T^h$ by solving the discrete variational problem

$$\langle V_T w_T^h, z_T^h \rangle = \langle (\tfrac{1}{2}I + K_T)u, z_T^h \rangle \qquad \forall z_T^h \in \mathcal{Z}_T^h.$$

A computable approximation to S_T is then given by

$$\widetilde{S}_T u := \alpha_T(D_T u + (\tfrac{1}{2}I + K_T')w_T^h).$$

It is easy to show that the approximation $\widetilde{S}_T$ remains self-adjoint and that its kernel is given by the constant functions, just as for S_T. Furthermore, the following spectral equivalence holds (see, e.g., [21, Sect. 7.1] or [20, Lemma 1.93]).

Theorem 3.1. *The element-level BEM-approximated Steklov-Poincaré operators $\widetilde{S}_T$ satisfy the spectral equivalence*

$$\tilde{c}_T \langle S_T v, v \rangle \leq \langle \widetilde{S}_T v, v \rangle \leq \langle S_T v, v \rangle \qquad \forall v \in H^{1/2}(\partial T) \qquad (3.2)$$

with a constant constant $\tilde{c}_T \in (0, \tfrac{1}{2})$ depending only on T.

Replacing, in (2.5), the exact Steklov-Poincaré operators S_T by their BEM approximations $\widetilde{S}_T$, we obtain the approximated bilinear form

$$\widetilde{a}(u,v) = \sum_{T \in \mathcal{T}} \langle \widetilde{S}_T u|_{\partial T}, v|_{\partial T} \rangle$$

and the inexact variational formulation: find $u \in H^{1/2}(\Gamma_S)$ with $u|_{\Gamma_D} = g_D$ such that

$$\widetilde{a}(u,v) = \langle F, v \rangle \qquad \forall v \in \mathcal{W}_D. \tag{3.3}$$

The constant $\tilde{c}_T$ from Theorem 3.1, while nonzero, depends on the geometry of the element T. For robust error estimates, it is required to bound $\tilde{c}_T$ from below uniformly for all elements. It is only recently that explicit bounds for these constants have been investigated, starting with a paper by Pechstein [21] which relied on the so-called Jones parameter and a constant in an isoperimetric inequality. These results were employed in the first rigorous *a priori* error analysis of the BEM-based FEM [10] as well as in a later analysis based on a mixed formulation which allowed to obtain L_2 error estimates [8]. Later, the assumptions were simplified such that, at least in the three-dimensional case, only relatively standard assumptions on mesh regularity have to be imposed [12, 9], which we state in the following.

Assumption 3.2. *There exists a shape-regular simplicial mesh $\Xi(\Omega')$ of an open, bounded superset $\Omega' \supset \overline{\Omega}$ of the computational domain Ω such that each element $T \in \mathcal{T}$ is the union of simplices from $\Xi(\Omega')$, and the number of simplices per element T is uniformly bounded. Furthermore, the boundary meshes $\mathcal{F}_T$ of ∂T, $T \in \mathcal{T}$ are uniformly shape-regular.*

Under these regularity assumptions, the following theorem holds.

Theorem 3.3 ([12, 9]). *Under Assumption 3.2 and for $d = 3$, the constants $\tilde{c}_T$, $T \in \mathcal{T}$, from (3.2) are uniformly bounded away from 0 by an expression which depends only on the mesh regularity parameters.*

Asssumption 3.2 can be slightly relaxed [12, Sect. 6]. We believe that Theorem 3.3 holds for $d = 2$ as well, but a proof is yet missing; see also [21].

4. Discretization

Due to the assumption that the local boundary meshes $\mathcal{F}_T$ are matching across element boundaries, $\mathcal{F} := \bigcup_{T \in \mathcal{T}} \mathcal{F}_T$ describes a shape-regular triangulation of the skeleton Γ_S. On this mesh, we construct the discrete trial spaces

$$\mathcal{W}_h := \left\{ v \in H^{1/2}(\Gamma_S) : v|_\tau \in P^1(\tau) \quad \forall \tau \in \mathcal{F} \right\}, \qquad \mathcal{W}_{h,0} := \mathcal{W}_h \cap \mathcal{W}_D$$

of piecewise linear, continuous functions on the skeleton. For simplicity, let us assume that g_D is continuous and piecewise linear with respect to the surface mesh. In that case, the discretized variational problem reads as follows: find $u_h \in \mathcal{W}_h$ with $u_h|_{\Gamma_D} = g_D$ such that

$$\widetilde{a}(u_h, v_h) = \langle F, v_h \rangle \qquad \forall v_h \in \mathcal{W}_{h,0}. \tag{4.1}$$

This is the variational formulation underlying the BEM-based FEM. Rigorous error estimates for this discretized variational problem may be found in
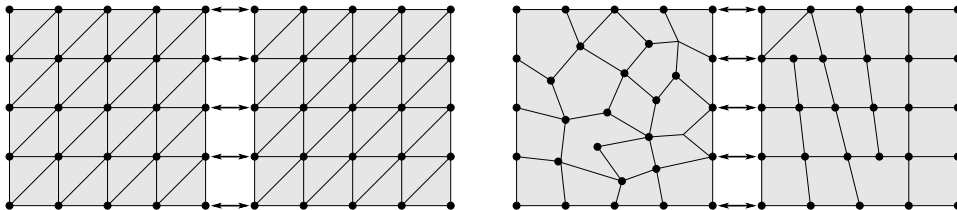
FIGURE 1. Sketch of domain decomposition approach in 2D for a rectangular domain with $N = 2$ subdomains. *Left:* FETI substructuring. *Right:* FETI-like substructuring for our BEM-based FEM.

[10, 8, 9]. They are of the same optimal order as a standard finite element method on an auxiliary finer mesh consisting of simplices.

Equivalently, (4.1) can be written as an operator equation

$$Au_h = F \qquad (4.2)$$

with $A : \mathcal{W}_h \to (\mathcal{W}_h)^*$. The associated stiffness matrix is given by

$$\underline{A} = (\langle A\phi_\ell, \, \phi_k \rangle)_{k,\ell},$$

where $\{\phi_k\}$ forms a nodal basis for $\mathcal{W}_{h,0}$ such that ϕ_k is 1 in the k-th skeletal node, 0 in all others, and interpolated linearly on every (simplicial) facet $\tau \in \mathcal{F}$ of the skeleton. It shares many properties with the stiffness matrix obtained from a standard finite element method in that it is sparse, symmetric, and positive definite.

5. A FETI SOLVER

In the following, we derive a solution method for (4.2) based on the ideas of the FETI substructuring approach, originally proposed by Farhat and Roux [7] and since then established both in theory and in practice as a highly efficient approach to the solution of discretized partial differential equations. Our derivation closely follows that of the classical FETI method, and we therefore refer to the literature, e.g., [7, 17, 13, 30, 20], for further details and some omitted proofs.

5.1. **Tearing and interconnecting.** We decompose the computational domain Ω into non-overlapping subdomains $(\Omega_i)_{i=1}^N$ in agreement with the polyhedral mesh $\mathcal{T}$, that is, $\overline{\Omega}_i = \bigcup_{T \in \mathcal{T}_i} \overline{T}$ with a corresponding decomposition $(\mathcal{T}_i)_{i=1}^N$. We set $H_i := \text{diam}(\Omega_i)$. Every subdomain Ω_i has an associated (fine) skeleton $\bigcup_{T \in \mathcal{T}_i} \partial T$ and a discrete skeletal trial space $\mathcal{W}_{h,0}(\Omega_i)$ as constructed in Section 4. In the following, we assume that the problem has been homogenized with respect to the given Dirichlet data g_D, so that $u_h \in \mathcal{W}_{h,0}$. It is easy to see that both the operator A and the functional F can be written as a sum of local contributions $A_i : \mathcal{W}_{h,0}(\Omega_i) \to \mathcal{W}_{h,0}(\Omega_i)^*$ given by

$$A_i u : v \mapsto \sum_{T \in \mathcal{T}_i} \langle \widetilde{S}_T u_T, \, v_T \rangle$$
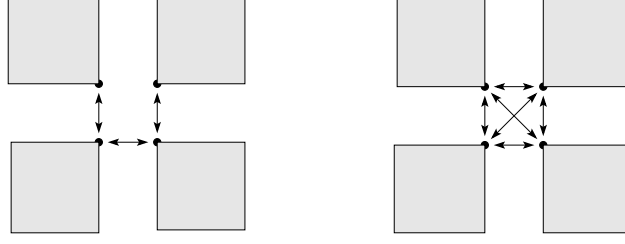
FIGURE 2. Constraints at the intersection between four sub-domains. *Left:* a choice of non-redundant constraints. *Right:* fully redundant constraints.

and, analogously, $\widetilde{F}_i \in \mathcal{W}_{h,0}(\Omega_i)^*$. We rewrite the global discrete problem (4.2) as the equivalent minimization problem

$$u = \underset{v \in \mathcal{W}_{h,0}(\Omega)}{\arg\min} \frac{1}{2} \sum_{i=1}^{N} \langle A_i v|_{\Omega_i}, v|_{\Omega_i} \rangle - \sum_{i=1}^{N} \langle \widetilde{F}_i, v|_{\Omega_i} \rangle, \qquad (5.1)$$

where above and in the sequel, we drop the subscript h since all functions are discrete from now on. Indeed, all relevant functions live in spaces of piecewise linear functions which have canonical nodal bases. Therefore, we will not distinguish in the following between functions and the coefficient vectors representing them with respect to the nodal basis, nor between operators and their matrix representations.

We group the degrees of freedom (dofs) on $\overline{\Omega}_i$ into *coupling* dofs (subscript Γ) that are associated with the *interface*

$$\Gamma := \bigcup_{i \neq j=1}^{N} (\partial\Omega_i \cap \partial\Omega_j) \setminus \overline{\Gamma}_D \,,$$

and the remaining *interior* dofs (subscript I). The latter are either in the interior of Ω_i or non-coupling dofs on the Neumann boundary Γ_N. Note that there are no dofs associated to the Dirichlet boundary Γ_D (for an alternative approach including Dirichlet dofs, see Remark 5.2 below).

For a discrete function $w_i \in \mathcal{W}_{h,0}(\Omega_i)$ with coupling dofs w_Γ and interior dofs w_I, the matrix A_i splits into blocks as well:

$$A_i w = \begin{bmatrix} A_{i,\Gamma\Gamma} & A_{i,\Gamma I} \\ A_{i,I\Gamma} & A_{i,II} \end{bmatrix} \begin{bmatrix} w_\Gamma \\ w_I \end{bmatrix}.$$

Eliminating the interior dofs leads to the Schur complement

$$\widetilde{S}_i = A_{i,\Gamma\Gamma} - A_{i,\Gamma I} A_{i,II}^{-1} A_{i,I\Gamma}.$$

Let $\Gamma_i := \partial\Omega_i \cap (\Gamma \cup \overline{\Gamma}_D)$ and let $\mathcal{W}_{h,0}(\Gamma_i)$ denote the trace space of $\mathcal{W}_{h,0}(\Omega_i)$ onto Γ_i, then $\widetilde{S}_i : \mathcal{W}_{h,0}(\Gamma_i) \to \mathcal{W}_{h,0}(\Gamma_i)^*$. The Schur complement system associated to (5.1) reads

$$u = \underset{v \in \mathcal{W}_{h,0}(\Gamma)}{\arg\min} \frac{1}{2} \sum_{i=1}^{N} \langle \widetilde{S}_i v|_{\Gamma_i}, v|_{\Gamma_i} \rangle - \sum_{i=1}^{N} \langle g_i, v|_{\Gamma_i} \rangle, \qquad (5.2)$$

where in matrix-vector notation, $g_i = \widetilde{F}_{i,\Gamma} - A_{i,\Gamma I} A_{i,II}^{-1} \widetilde{F}_{i,I}$, cf. [30, Sect. 4.3].

We introduce a space Y of broken functions, given by

$$Y_i := \mathcal{W}_{h,0}(\Gamma_i), \qquad Y := \prod_{i=1}^{N} Y_i.$$

Functions from Y may have two different values on either side of a sub-domain interface. Only if their values match across interfaces can they be identified with functions in $\mathcal{W}_{h,0}(\Gamma \cup \overline{\Gamma}_D)$. In order to enforce this, we intro-duce the jump operator $B : Y \to \mathbb{R}^{N_\Lambda}$, where $N_\Lambda \in \mathbb{N}$ is the total number of constraints. In the nodal basis, B has exactly two non-zero contributions of opposite sign per constraint and may thus be viewed as a signed Boolean matrix. In this work, we assume fully redundant constraints [24], i.e., for every node on a subdomain interface, constraints corresponding to all neigh-boring subdomains are introduced. This is in contrast to the non-redundant case, where only a minimal set of constraints is introduced in order to en-sure continuity, see Figure 2 for an illustration. The choice of redundant constraints implies that the jump operator B is not surjective. As common in the literature, we define the space of Lagrange multipliers as

$$\Lambda := \mathrm{range}(B) \subseteq \mathbb{R}^{N_\Lambda}$$

and consider B as a mapping $Y \to \Lambda$ in the following. Alternatively, one could define Λ as the factor space $\mathbb{R}^{N_\Lambda}$ modulo $\ker(B^\top)$.

The jump operator B can be written as a sum of local contributions $B_i : Y_i \to \Lambda$, and the globally consistent functions in Y are those which satisfy

$$By = \sum_{i=1}^{N} B_i y_i = 0,$$

that is, $y \in \ker(B)$. In light of this, we rewrite (5.2) as

$$u = \underset{\substack{y \in Y \\ By=0}}{\arg\min} \frac{1}{2} \sum_{i=1}^{N} \langle \widetilde{S}_i y_i, \, y_i \rangle - \sum_{i=1}^{N} \langle g_i, \, y_i \rangle.$$

Introducing Lagrange multipliers to enforce the constraint $By = 0$, we obtain the saddle point formulation

$$\text{find } (u, \lambda) \in Y \times \Lambda : \quad \begin{bmatrix} \widetilde{S} & B^\top \\ B & 0 \end{bmatrix} \begin{bmatrix} u \\ \lambda \end{bmatrix} = \begin{bmatrix} g \\ 0 \end{bmatrix}, \tag{5.3}$$

where we have used the block matrices and vectors $\widetilde{S} = \mathrm{diag}(\widetilde{S}_1, \ldots, \widetilde{S}_N)$, $B = (B_1, \ldots, B_N)$, $u = (u_1, \ldots, u_N)^\top$, $g = (g_1, \ldots, g_N)^\top$.

5.2. **Elimination of the primal unknowns** u. From (5.3), we see that the local skeletal functions u_i satisfy the relationship

$$\widetilde{S}_i u_i = g_i - B_i^\top \lambda. \tag{5.4}$$

For a *non-floating* subdomain Ω_i, where $\partial\Omega_i \cap \Gamma_D \neq \emptyset$, the operator $\widetilde{S}_i$ is positive definite and thus invertible. For a *floating* subdomain Ω_i, where $\partial\Omega_i \cap \Gamma_D = \emptyset$, the kernel of $\widetilde{S}_i$ consists of the constant functions. In the latter case, we select an injective operator R_i with $\mathrm{range}(R_i) = \ker(\widetilde{S}_i)$, e.g.,

$$R_i : \mathbb{R} \to \ker(\widetilde{S}_i) \subseteq Y_i : \xi_i \mapsto \xi_i.$$

Under the condition that the right-hand side is orthogonal to the kernel, i.e.,

$$\langle g_i - B_i^\top \lambda,\, R_i \zeta \rangle = 0 \qquad \forall \zeta \in \mathbb{R}, \tag{5.5}$$

the local problem (5.4) is solvable. Let $\widetilde{S}_i^\dagger$ denote a generalized inverse of $\widetilde{S}_i$, with the minimal requirement that

$$\widetilde{S}_i \widetilde{S}_i^\dagger f = f \qquad \forall f \in \text{range}(\widetilde{S}_i).$$

Then, under condition (5.5),

$$u_i = \widetilde{S}_i^\dagger (g_i - B_i^\top \lambda) + R_i \xi_i \tag{5.6}$$

with some $\xi_i \in \mathbb{R}$. A simple choice for the generalized inverse is

$$\widetilde{S}_i^\dagger = (\widetilde{S}_i + \beta_i R_i R_i^\top)^{-1}$$

for some $\beta_i > 0$. For practical reasons, different choices are usually preferred, see e.g., [7, Appendix I] and [20, Sect. 1.2.5.2]. In particular, one usually factorizes a part or a regularization of the *original* matrix A_i to stay in the regime of sparse matrices [30, Sect. 1.3], see also Remark 5.1 below. Note, however, that the algorithm and analysis below are independent of the actual choice of $\widetilde{S}_i^\dagger$.

Formulae (5.5) and (5.6) remain valid for non-floating subdomains Ω_i, if we set $R_i \equiv 0$ and $\widetilde{S}_i^\dagger = \widetilde{S}_i^{-1}$. Hence, with $Z := \prod_{i=1}^N \mathbb{R}^{\dim(\ker(\widetilde{S}_i))}$ and the block operators $R = \text{diag}(R_1, \ldots, R_N) : Z \to Y$ and $\widetilde{S}^\dagger = \text{diag}(\widetilde{S}_1^\dagger, \ldots, \widetilde{S}_N^\dagger)$, the local solutions u can be expressed by

$$u = \widetilde{S}^\dagger (g - B^\top \lambda) + R\xi, \qquad \text{for some } \xi \in Z, \tag{5.7}$$

under the compatibility condition (derived from (5.5))

$$R^\top B^\top \lambda = R^\top g.$$

Inserting (5.7) into the second line of (5.3) yields $B\widetilde{S}^\dagger g - B\widetilde{S}^\dagger B^\top \lambda + BR\xi = 0$. Together with the compatibility condition, and with $F := B\widetilde{S}^\dagger B^\top$ and $G := BR$, we obtain the dual saddle point problem

$$\text{find } (\lambda, \xi) \in \Lambda \times Z : \quad \begin{bmatrix} F & -G \\ G^\top & 0 \end{bmatrix} \begin{bmatrix} \lambda \\ \xi \end{bmatrix} = \begin{bmatrix} B\widetilde{S}^\dagger g \\ R^\top g \end{bmatrix}. \tag{5.8}$$

5.3. **Projection method.** Problem (5.8) is now solved using the projection method. With a self-adjoint operator $Q : \Lambda \to \Lambda$ (yet to be specified) which is positive definite on the range of G, we define

$$P = I - QG(G^\top Q G)^{-1} G^\top.$$

It is easy to see that $G^\top Q G$ is positive definite and thus indeed invertible, and that P is a projection from Λ onto the subspace

$$\Lambda_0 := \ker(G^\top) \subseteq \Lambda.$$

The particular vector $\lambda_g := QG(G^\top Q G)^{-1} R^\top g \in \Lambda$ fulfills the constraint $G^\top \lambda_g = R^\top g$ by construction. Thus, with $\lambda = \lambda_0 + \lambda_g$, we can homogenize (5.8) such that we only need a Lagrange parameter $\lambda_0 \in \Lambda_0$ fulfilling

$$F\lambda_0 - G\xi = \underbrace{B\widetilde{S}^\dagger g - F\lambda_g}_{B\widetilde{S}^\dagger (g - B^\top \lambda_g)}. \tag{5.9}$$

Applying the projector $P^\top$ to this equation and noting that $P^\top G = 0$, we are left to

$$\text{find } \lambda_0 \in \Lambda_0 : \quad P^\top F \lambda_0 = P^\top B \widetilde{S}^\dagger (g - B^\top \lambda_g). \qquad (5.10)$$

It can be shown that $P^\top F$ is self-adjoint and positive definite on Λ_0, and so system (5.10) has a unique solution which may be computed by a conjugate gradient (CG) iteration in the subspace Λ_0. Once $\lambda = \lambda_0 + \lambda_g$ has been computed, ξ can be retrieved from the formula

$$\xi = (G^\top Q G)^{-1} G^\top Q B \widetilde{S}^\dagger (B^\top \lambda - g),$$

which is obtained by applying $(G^\top Q G)^{-1} G^\top Q$ to (5.9). Finally, the original unknowns u_i are obtained by formula (5.7).

Remark 5.1. *The initial elimination of interior dofs in Sect. 5.1 is done mainly for theoretical reasons and will be used in the analysis below. In practice, one usually works with the original matrices A_i and suitable generalized inverses $A_i^\dagger$ rather than with $\widetilde{S}_i$, $\widetilde{S}_i^\dagger$ (at least for the operators defined in Sect. 5.1–Sect. 5.3). However, whether with or without the elimination, the resulting systems (5.8) and (5.10) remain the same, cf. [25, Sect. 2.1.3], [20, Rem. 2.17].*

Remark 5.2. *In contrast to the original FETI approach, the* total FETI *(TFETI) [4] and the* all-floating BETI *[19] techniques include Dirichlet boundary dofs from the start and enforce the Dirichlet conditions by Lagrange multipliers as well. This results in the fact that all subdomains are floating in the sense that every subdomain matrix has a one-dimensional kernel, and that the "coarse" matrix $G^\top Q G$ is slightly larger than in classical FETI, see also [21, Sect. 2.2.2]. The all-floating approach can of course be used for the BEM-based FETI as well and leads to analogous results.*

5.4. **Preconditioning.** Preconditioners for FETI are typically constructed in the form PM^{-1} with a suitable operator $M^{-1} : \Lambda \to \Lambda$. The Dirichlet preconditioner proposed by Farhat, Mandel, and Roux [6], adapted to our setting, is given by the choice

$$M^{-1} = B \widetilde{S} B^\top$$

and works well for globally constant or mildly varying coefficient α. In this case, the choice $Q = I$ works satisfactorily.

To deal with coefficient jumps, we need to employ a *weighted* or *scaled jump operator* as introduced by Rixen and Farhat [24] in a mechanical setting and later analyzed by Klawonn and Widlund [13] for the scalar potential equation. For this, let $x^h \in \partial\Omega_i$ refer to an arbitrary boundary node and introduce scalar weights $\rho_i(x^h) > 0$. We will restrict ourselves to the case of subdomain-wise constant coefficient α in the following, i.e.,

$$\alpha(x) = \alpha_i \qquad \forall x \in \Omega_i.$$

For a comprehensive treatment of the case of an unresolved diffusion coefficient, we refer to [22, 23, 20]. In the setting of piecewise constant α, we simply choose the weights

$$\rho_i(x^h) = \alpha_i.$$

These are used to define the *weighted counting functions* $\delta_j^\dagger$, $j = 1, \ldots, N$, by the nodal values

$$\delta_j^\dagger(x^h) := \begin{cases} \dfrac{\rho_j(x^h)}{\sum_{k \in \mathcal{N}(x^h)} \rho_k(x^h)} & \text{if } x^h \in \partial\Omega_j, \\ 0 & \text{if } x^h \in \overline{\Gamma} \setminus \partial\Omega_j, \end{cases}$$

and piecewise linear interpolation on the facets of $\overline{\Gamma}$. Above, $\mathcal{N}(x^h) = \{i \in \{1, \ldots, N\} : x^h \in \partial\Omega_i\}$ is the set of subdomains on whose boundaries x^h lies. The family of counting functions $\{\delta_j^\dagger\}_{j=1}^N$ forms a partition of unity on $\overline{\Gamma}$. If α is globally constant, then $\delta_j^\dagger(x^h)$ is the reciprocal of the multiplicity of x^h, and hence often called *multiplicity scaling*.

Following [24, 13], we introduce diagonal scaling matrices $D_i : \Lambda \to \Lambda$, $i = 1, \ldots, N$, operating on the space of Lagrange multipliers. Consider two neighboring domains Ω_i and Ω_j sharing a node $x^h \in \partial\Omega_i \cap \partial\Omega_j$. Let $k \in \{1, \ldots, N_\Lambda\}$ denote the index of the Lagrange multiplier associated with this node and pair of subdomains. Then, the k-th diagonal entry of D_i is set to $\delta_j^\dagger(x^h)$, and the k-th diagonal entry of D_j is set to $\delta_i^\dagger(x^h)$. Diagonal entries of D_i not associated with a node on $\partial\Omega_i$ are set to zero.

The *scaled jump operator* $B_D : Y \to \Lambda$ is now given by

$$B_D = [D_1 B_1, \ldots, D_N B_N],$$

and the scaled Dirichlet preconditioner by

$$M_D^{-1} = B_D \widetilde{S} B_D^\top.$$

In this case, a possible choice for Q is simply $Q = M_D^{-1}$. Alternatively, Q can be replaced by a suitable diagonal matrix as described in [13].

6. Convergence analysis

In this subsection, we first construct auxiliary subdomain meshes together with corresponding standard finite element (FE) spaces and matrices. We then prove element- and subdomain-wise spectral equivalence relations between the FE and the BEM-based FEM matrices. This approach allows to lift known results of classical FETI to BEM-based FETI.

6.1. **Auxiliary simplicial meshes and FE matrices.** For each subdomain Ω_i, we consider a simplicial, shape-regular mesh Ξ_i of Ω_i such that

(i) each polytopal element in $\mathcal{T}_i$ is a union of simplices from Ξ_i,
(ii) for each element $T \in \mathcal{T}_i$, the restriction of the surface mesh $\mathcal{F}_T$ to $\partial\Omega_i$ and the restriction of the volume Ξ_i to $\partial\Omega_i \cap \partial T$ are identical, and
(iii) the number of simplices per polytopal element is uniformly bounded.

Thanks to Assumption 3.2, such meshes indeed exist.

On each auxiliary mesh Ξ_i, we construct the standard piecewise linear finite element space $\mathcal{V}_h(\Omega_i)$ as well as $\mathcal{V}_{h,0}(\Omega_i) := \{w \in \mathcal{V}_h(\Omega_i) : w|_{\Gamma_D} = 0\}$. We note that, by construction, the space Y_i introduced in Sect. 5.1 is simply the trace space of $\mathcal{V}_{h,0}(\Omega_i)$ onto $\partial\Omega_i$. In the following, the letter $\mathcal{V}$ will always

be used for finite element spaces associated to Ξ_i, whereas the letter $\mathcal{W}$ will be associated with spaces of functions living on boundaries or skeletons.

Recall that every element $T \in \mathcal{T}_i$ is the union of simplices from Ξ_i. On each such *macroelement* $T \in \mathcal{T}_i$, we assemble the local stiffness matrix K_T^{F},

$$\langle K_T^{\mathrm{F}} v, \, w \rangle = \sum_{\gamma \in \Xi_i, \gamma \subseteq T} \int_\gamma \alpha \nabla v \cdot \nabla w \, dx \qquad \text{for } v, w \in \mathcal{V}_{h,0}(T).$$

The superscript F stands for standard "FEM". Static condensation of possible dofs in K_T^{F} that are not associated to ∂T leads to the Schur complement

$$S_T^{\mathrm{F}} : \mathcal{W}_{0,h}(\partial T) \to \mathcal{W}_{0,h}(\partial T)^*,$$

where $\mathcal{W}_{0,h}(\partial T)$ is the trace space of $\mathcal{V}_{0,h}(\Omega_i)$ on ∂T, which—due to Property (ii) above—is identical to the restriction of the space $\mathcal{W}_{0,h}(\Omega_i)$ from Sect. 5.1 to ∂T.

6.2. **Spectral equivalence relations.** In this subsection, we derive spectral equivalence relations between several FEM and BEM-based FEM matrices. To simplify the notation, for symmetric matrices A and $B \in \mathbb{R}^n$, we write $A \cong B$ for

$$c \langle Aw, \, w \rangle \leq \langle Bw, \, w \rangle \leq C \langle Aw, \, w \rangle \qquad \forall w \in \mathbb{R}^n,$$

if the (positive) equivalence constants c, C depend only on mesh regularity parameters of Assumption 3.2. Throughout this subsection, we assume $d = 3$ in view of Theorem 3.3.

Lemma 6.1. *Let Assumption 3.2 be fulfilled. Then for each (macro)element $T \in \mathcal{T}_i$,*

$$S_T^{\mathrm{F}} \cong \widetilde{S}_T \, .$$

Proof. Recall the local, exact Steklov-Poincaré operator S_T from Sect. 3. In [20, Corollary 1.57], it is shown that

$$\langle S_T v, \, v \rangle \leq \langle S_T^{\mathrm{F}} v, \, v \rangle \leq C \langle S_T v, \, v \rangle \qquad \forall v \in \mathcal{W}_{h,0}(\partial T),$$

where the constant C only depends on the shape regularity constant of Ξ_i. The proof in [20] is written down for $\alpha_T = 1$ but generalizes straighforwardly, because both S_T and S_T^{F} scale linearly in α_T. The lower bound with a factor of 1 is due to the fact that S_T minimizes the energy over extensions $\widetilde{v} \in H^1(T)$ whereas S_T^{F} over $\widetilde{v} \in \mathcal{V}_{h,0}(T)$ with $\widetilde{v}|_{\partial T} = v$. The constant in the upper bound originates from the stability estimate

$$|\Pi_T u|^2_{H^1(T)} \leq C \, |u|^2_{H^1(T)} \qquad \forall u \in H^1(T)$$

of the Scott-Zhang operator Π_T [28], which can be chosen such that Π_T preserves piecewise linear boundary data on ∂T. The assertion now follows from Theorem 3.1 (stating that $\widetilde{S}_T \cong S_T$ on $\mathcal{W}_{h,0}(\partial T)$) and transitivity. $\square$

For each subdomain Ω_i, we assemble the local condensed stiffness matrices S_T^{F} over $T \in \mathcal{T}_i$ resulting in the matrix $K_i^{\mathrm{F},S}$, given by

$$\langle K_i^{\mathrm{F},S} v, \, w \rangle = \sum_{T \in \mathcal{T}_i} \langle S_T^{\mathrm{F}} v|_{\partial T}, \, w|_{\partial T} \rangle \qquad \forall v \in \mathcal{W}_{0,h}(\Omega_i).$$

As we did for the matrix A_i in Sect. 5.1, we eliminate all the *interior* dofs from $K_i^{F,S}$, which results in the Schur complement

$$S_i^{F} : \mathcal{W}_{0,h}(\partial\Omega_i) \to \mathcal{W}_{0,h}(\partial\Omega_i)^*.$$

Lemma 6.2. *Under Assumption 3.2, for each* $i = 1, \ldots, N$,

$$A_i \cong K_i^{F,S} \quad and \quad \widetilde{S}_i \cong S_i^{F}.$$

Proof. Recall that

- $K_i^{F,S}$ assembles the matrices S_T^{F} over $T \in \mathcal{T}_i$ and S_i^{F} is the Schur complement of $K_i^{F,S}$,
- A_i assembles the matrices $\widetilde{S}_T$ over $T \in \mathcal{T}_i$ and $\widetilde{S}_i$ is the Schur complement of A_i.

Since $S_T^{F} \cong \widetilde{S}_T$ (Lemma 6.1), the first spectral equivalence is obtained immediately by summing over $T \in \mathcal{T}_i$. The second equivalence holds because corresponding Schur complements of spectrally equivalent matrices are again spectrally equivalent. $\qquad\square$

The spectral equivalence from Lemma 6.2 above implies a similar equivalence for generalized inverses of the BEM-based FEM Schur complement $\widetilde{S}_i$ and the FEM Schur complement S_i^{F}.

Lemma 6.3. *Let Assumption 3.2 hold and let* $(S_i^{F})^\dagger$ *be any generalized inverse of* S_i^{F}, *such that* $S_i^{F}(S_i^{F})^\dagger f = f$ *holds for all* $f \in \mathrm{range}(S_i^{F})$. *Then*

$$\widetilde{S}_i^\dagger \cong (S_i^{F})^\dagger \quad on \ \mathrm{range}(\widetilde{S}_i).$$

Proof. Recall from Lemma 6.2 that $S_i^{F} \cong \widetilde{S}_i$. Moreover, both matrices are symmetric and positive semi-definite and

$$\ker(S_i^{F}) = \ker(\widetilde{S}_i), \qquad \mathrm{range}(S_i^{F}) = \mathrm{range}(\widetilde{S}_i).$$

The assumptions on the generalized inverses yield that for $f \in \mathrm{range}(\widetilde{S}_i)$, we have $\widetilde{S}_i^\dagger = (\widetilde{S}_{i/\ker(\widetilde{S}_i)})^{-1} + \xi$ for some $\xi \in \ker(\widetilde{S}_i)$. Since $\mathrm{range}(\widetilde{S}_i)$ is orthogonal to $\ker(\widetilde{S}_i)$, we have

$$\langle f, \widetilde{S}_i^\dagger f \rangle = \langle f, (\widetilde{S}_{i/\ker(\widetilde{S}_i)})^{-1} f \rangle \qquad \forall f \in \mathrm{range}(\widetilde{S}_i).$$

The analogous property holds for $(S_i^{F})^\dagger$. Due to simple algebraic argument, $S_i^{F} \cong \widetilde{S}_i$ implies $(\widetilde{S}_{i/\ker(\widetilde{S}_i)})^{-1} \cong (S_{i/\ker(S_i^{F})}^{F})^{-1}$. Summarizing, $\langle f, \widetilde{S}_i^\dagger f \rangle \cong \langle (S_i^{F})^\dagger f, f \rangle$ for all $f \in \mathrm{range}(\widetilde{S}_i)$, which concludes the proof. $\qquad\square$

6.3. **Condition number estimates for BEM-based FETI.** To prove condition number estimates for the BEM-based FETI, we make use of the classical FETI theory.

Recall that the matrix S_i^{F} from Sect. 6.2 is constructed from the classical FE stiffness matrix on $\mathcal{V}_{0,h}(\Omega_i)$ by *two* elimination steps: firstly the static condensation of dofs not associated to ∂T and secondly the elimination of interior dofs. It is easily seen that the elimination of *all* the interior dofs of $\mathcal{V}_{h,0}(\Omega_i)$ *together* results in the same matrix S_i^{F}. In other words, S_i^{F} is the classical Schur complement of the subdomain FE stiffness matrix (based on Ξ_i) which is used in classical FETI.

We select generalized inverses $(S_i^{\mathrm{F}})^{\dagger}$ of S_i^{F} and set $(S^{\mathrm{F}})^{\dagger} := \mathrm{diag}((S_i^{\mathrm{F}})^{\dagger})_{i=1}^N$. Due to Property (ii) in Sect. 6.1, the meshes $\mathcal{T}_i$ and Ξ_i coincide on $\partial\Omega_i$. Consequently, the operators B and B_D defined above are exactly those from the classical FETI algorithm. The standard FETI operator is given by

$$F^{\mathrm{F}} := B(S^{\mathrm{F}})^{\dagger} B^{\top}.$$

Since S_i^{F} and $\widetilde{S}_i$ have identical kernel and range, the operators G, P, Q, and R defined above coincide with those from classical FETI as well.

The unpreconditioned case. The following result is known from the FETI literature.

Assumption 6.4 ([30, Ass. 4.3]).   1. *Each subdomain Ω_i is the union of a few simplices from a conforming and shape-regular coarse triangulation of Ω.*
  2. *The set $\partial\Omega_i \cap \Gamma_D$ is either empty or a union of vertices, edges, or faces of the above coarse triangulation.*

Theorem 6.5 ([6, 20]). *Suppose that Assumption 6.4 holds and that for each $i = 1, \ldots, N$, the restriction of Ξ_i to $\partial\Omega_i$ is quasi-uniform with mesh parameter h_i^{F}. Moreover, assume that $\partial\Omega_i \cap \Gamma_D$ is either empty or has positive surface measure. Then, for the choice $Q = I$, the classical FETI operator satisfies the condition number estimate*

$$\kappa(P^{\top} F^{\mathrm{F}}|_{\Lambda_0}) \leq C \frac{\overline{\alpha}}{\underline{\alpha}} \Big(\max_{i=1,\ldots,N} \frac{H_i}{h_i^{\mathrm{F}}} \Big),$$

where $H_i = \mathrm{diam}(\Omega_i)$, $\overline{\alpha} = \max_{x\in\Omega} \alpha(x)$, $\underline{\alpha} = \min_{x\in\Omega} \alpha(x)$, and C depends only on the mesh regularity parameters of Assumption 6.4.

Using the spectral equivalence relations from Sect. 6.2, we are able to lift the above condition number estimate for the classical FETI operator $P^{\top} F^{\mathrm{F}}$ to one for the BEM-based FETI operator $P^{\top} F$.

Theorem 6.6. *Let $d = 3$, let Assumption 3.2 and Assumption 6.4 hold, and suppose that for each $i = 1, \ldots, N$, the restriction of $\mathcal{T}_i$ to $\partial\Omega_i$ is a quasi-uniform triangulation (with mesh parameter h_i). Moreover, assume that $\partial\Omega_i \cap \Gamma_D$ is either empty or has positive surface measure. Then, for the choice $Q = I$,*

$$\kappa(P^{\top} F|_{\Lambda_0}) \leq C \frac{\overline{\alpha}}{\underline{\alpha}} \Big(\max_{i=1,\ldots,N} \frac{H_i}{h_i} \Big),$$

where $\overline{\alpha} = \max_{x\in\Omega} \alpha(x)$, $\underline{\alpha} = \min_{x\in\Omega} \alpha(x)$, and C depends only on the mesh regularity parameters of Assumptions 3.2 and 6.4.

Proof. Step 1: we show that the operator $P^{\top} F$ and its classical FETI analogue $P^{\top} F^{\mathrm{F}}$ are spectrally equivalent on the subspace Λ_0. Since P is a projector onto Λ_0, we have

$$\langle P^{\top} F\lambda, \lambda \rangle = \langle F\lambda, \lambda \rangle \quad \text{and} \quad \langle P^{\top} F^{\mathrm{F}}\lambda, \lambda \rangle = \langle F^{\mathrm{F}}\lambda, \lambda \rangle \qquad \forall \lambda \in \Lambda_0.$$

From $G = GR$, $\mathrm{range}(R) = \ker(\widetilde{S}) = \ker(\widetilde{S}^{\mathrm{F}})$ the fact that $\mathrm{range}(\widetilde{S})$ is spanned by the vectors orthogonal to $\ker(\widetilde{S})$, we see that

$$\Lambda_0 = \ker(G^{\top}) = \{\lambda \in U : B^{\top}\lambda \in \mathrm{range}(\widetilde{S})\}.$$

Hence, from the definitions of F and F^{F}, the above properties, and Lemma 6.3, it follows that

$$\langle P^\top F\lambda,\,\lambda\rangle = \langle \widetilde{S}^\dagger B^\top\lambda,\, B^\top\lambda\rangle \cong \langle \widetilde{(S^{\mathrm{F}})^\dagger} B^\top\lambda,\, B^\top\lambda\rangle = \langle P^\top F^{\mathrm{F}}\lambda,\,\lambda\rangle \quad \forall\lambda\in\Lambda_0,$$

where the hidden constants only depend on the mesh regularity parameters of Assumption 3.2. In other words, $P^\top F \cong P^\top F^{\mathrm{F}}$ on Λ_0.

Step 2: due to Property (ii) in Sect. 6.1, $h_i \cong h_i^{\mathrm{F}}$. The assertion now follows straightforwardly from Theorem 6.5 and the spectral equivalence of Step 1. $\square$

The preconditioned case. In a similar fashion to the above, we transfer the known results on the condition number of the FETI system preconditioned with the scaled Dirichlet preconditioner to our setting. For simplicity, we do this for a subdomain-wise constant diffusion coefficient, where $\alpha(x) = \alpha_i$ for all $x \in \Omega_i$. However, all the available theoretical results for non-resolved coefficients [22, 23, 20] can be transferred to BEM-based FETI, see Remark 6.8 below. In particular, as the simplest of all generalizations, if we set $\rho_i(x^h) := \overline{\alpha}_i$ for all $x^h \in \partial\Omega_i \cap \Gamma$, then all the statements below hold as well with an additional factor of $\max_{i=1}^N \overline{\alpha}_i/\underline{\alpha}_i$.

Theorem 6.7. *Let $d = 3$, let Assumption 3.2 and Assumption 6.4 hold, and assume additionally that $\partial\Omega_i \cap \Gamma_D$ is either empty or contains at least an edge of the coarse triangulation from Assumption 6.4. Moreover, suppose that $\alpha(x) = \alpha_i = const$ for $x \in \Omega_i$. Then, for the choice $Q = M_D^{-1}$, we have the condition number estimate*

$$\kappa(PM_D^{-1}P^\top F|_{\Lambda_0}) \le C \max_{i=1,\dots,N}(1 + \log(H_i/h_i))^2,$$

where C depends only on the mesh regularity parameters of Assumptions 3.2 and 6.4. In particular, C is independent of H_i, h_i, the number of subdomains, and of the values α_i.

Proof. In the first part of this proof, we follow the abstract, algebraic part of the classical FETI analysis (see e.g., [30]), which can be carried out verbatim for our setting of BEM-based FEM. Following the steps of the proofs of [20, Lemma 2.42, Lemma 2.43], we see that M_D^{-1} is positive definite on $\mathrm{range}(P^\top)$, which is isomorphic to the dual of Λ_0. Therefore, to obtain a condition number bound of the form $\kappa(PM_D^{-1}P^\top F|_{\Lambda_0}) \le c_2/c_1$, it suffices to show that

$$c_1\langle M_D\lambda,\,\lambda\rangle \le \langle F\lambda,\,\lambda\rangle \le c_2\langle M_D\lambda,\,\lambda\rangle \qquad \forall\lambda\in\Lambda_0, \tag{6.1}$$

where M_D is the inverse of $M_D^{-1}|_{\mathrm{range}(P^\top)}$. For the choice $Q = M_D^{-1}$, following the steps of [30, Theorem 6.15] in a purely algebraic fashion, one obtains the lower bound with $c_1 = 1$. Similarly, by following the steps of [30, Sect. 6.3.3] or [20, Sect. 2.4.2.3 and Sect. 2.6] in a purely algebraic fashion, one obtains the following result. Fix subspaces $Y_i^\perp \subseteq Y_i$ with codimension $\dim(\ker(\widetilde{S}_i^{\mathrm{F}}))$, e.g., by restricting a suitable mean value to zero if Ω_i is floating, and set $Y := \prod_{i=1}^N Y_i$. Then, for $Q = M_D^{-1}$, an estimate of the form

$$|B_D^\top By|_{\widetilde{S}}^2 \le \omega|y|_{\widetilde{S}}^2 \qquad \forall y \in Y^\perp \tag{6.2}$$

implies the upper bound in (6.1) with $c_2 = 4\omega$. For the classical FETI setting, it was shown in [13] that

$$|B_D^\top B y|_{S^F}^2 \leq C \max_{i=1,\ldots,N} (1 + \log(H_i/h_i^F))^2 |y|_{S^F}^2 \qquad \forall y \in Y^\perp. \qquad (6.3)$$

The constant C depends only on the mesh regularity parameters from Assumption 6.4 and from the shape-regularity and quasi-uniformity constants of Ξ_i restricted to $\partial\Omega_i$, cf. [20]. Due to the established spectral equivalence $S^F \cong \widetilde{S}$ from Lemma 6.2 and since $h_i \cong h_i^F$, estimate (6.3) implies (6.2) and the upper bound in (6.1) with $c_2 \cong \omega \cong \max_{i=1,\ldots,N}(1 + \log(H_i/h_i))^2$. $\qquad\square$

Remark 6.8.   1. *In [13], a diagonal choice of Q is proposed and analyzed for classical FETI, leading to the same condition number estimate as in Theorem 6.5. The entries of this diagonal Q only include the values α_i, $h_i^F \cong h_i$, and H_i, $i = 1,\ldots,N$. Because of the established spectral equivalence $S^F \cong \widetilde{S}$, the diagonal choice for Q in the setting of BEM-based FETI leads to the same condition number estimate as in Theorem 6.7.*

2. *If the assumption on the piecewise constant diffusion coefficient is dropped, then still, Lemma 6.2 allows to lift the results in [20, Ch. 3] to the case of BEM-based FETI, for both the case $Q = M_D^{-1}$ as well as for suitable diagonal choices of Q [20, Sect. 3.3.5.4].*

3. *The assumption $d = 3$ in Theorem 6.6 and Theorem 6.7 could be dropped, if the statement of Theorem 3.3 held (provably) for $d = 2$.*

4. *The spectral equivalence relation of Lemma 6.2 allows to lift the known condition number estimates of Neumann-Neumann, FETI-DP, and BDDC methods from FEM to BEM-based FEM in a similar fashion.*

7. NUMERICAL EXPERIMENTS

To demonstrate the behavior of the described algorithm, we solve the Laplace equation with pure Dirichlet boundary conditions,

$$-\Delta u = 0 \quad \text{in } \Omega, \qquad u(x) = -\frac{1}{2\pi}\log|x - x^\star| \quad \text{on } \partial\Omega,$$

on a two-dimensional domain Ω (Figure 3, left) which is discretized by an irregular polygonal mesh. The source point $x^\star = (-1, 1)^\top$ lies outside of Ω.

The polygonal mesh $\mathcal{T}$ is constructed by applying METIS to a standard triangular mesh consisting of 524,288 triangles, resulting in a polygonal mesh with 99,970 elements, most of which are unions of 5 or 6 triangles. A few of these elements are shown in the closeup in Figure 3, right.

The domain decomposition $\{\Omega_i\}$ is obtained by applying METIS a second time on top of the mesh $\mathcal{T}$. The result of this step is shown in Figure 3, left, for the case of $N = 100$ subdomains.

We use the Dirichlet preconditioner with multiplicity scaling and a suitable diagonal matrix for Q as described in [13] for ease of implementation. The preconditioned equation

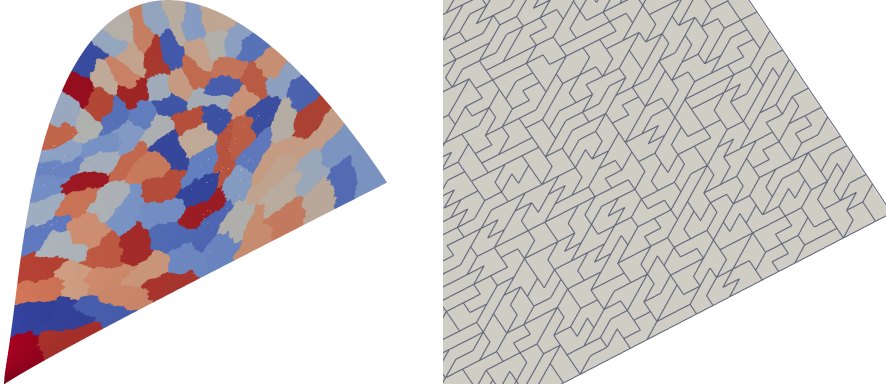$$PM_D^{-1}P^\top F\lambda_0 = PM_D^{-1}\tilde{g}$$

FIGURE 3. *Left:* Computational domain with a sample partitioning of $N = 100$ subdomains. *Right:* Detail of polygonal mesh at right domain corner.

is solved by preconditioned Conjugate Gradient (PCG) iteration. In the following, we give the number of PCG iterations required to achieve reduction of the initial residual by a factor of 10^{-8} for varying number N of subdomains. We also compare these results to the non-preconditioned equation (5.10) solved by standard CG iteration. The estimated condition numbers and iteration numbers for the non-preconditioned and the preconditioned case, respectively, are shown in Figures 4 and 5. Additional data on these two cases can be found in Tables 1 and 2, respectively.

We point out that the jagged nature of the plots in Figures 4 and 5 is due the fact that the domain decompositions were individually created by METIS for varying N and therefore not nested. The non-preconditioned case, Figure 4, shows a decay in the condition number which roughly correlates to the theoretical estimate from Theorem 6.6, $\kappa = \mathcal{O}(H/h) = \mathcal{O}(N^{-1/2})$. The condition numbers for the preconditioned case in Figure 5 show no clear tendency, which may be due to the problem size being too small. Most importantly, they stay uniformly bounded, and therefore so do the iteration numbers. We have compared the condition and iteration numbers to an analogous FETI method for a Courant FEM on the underlying triangular mesh, and the numbers are comparable, indicating that the behavior of the condition number is not particular to the BEM-based FEM.

8. CONCLUSION AND OUTLOOK

We have applied a FETI-like solution scheme to the setting of a BEM-based FEM and have shown that it results in a solver with performance comparable to that of standard FETI solvers for FEM discretizations. Two different preconditioners for the case of low and high variation in the diffusion coefficients, respectively, have likewise been transferred to this setting. By proving a spectral equivalence for Schur complements on the subdomain level, we succeeded in proving condition number estimates equivalent to those known from the FETI literature.
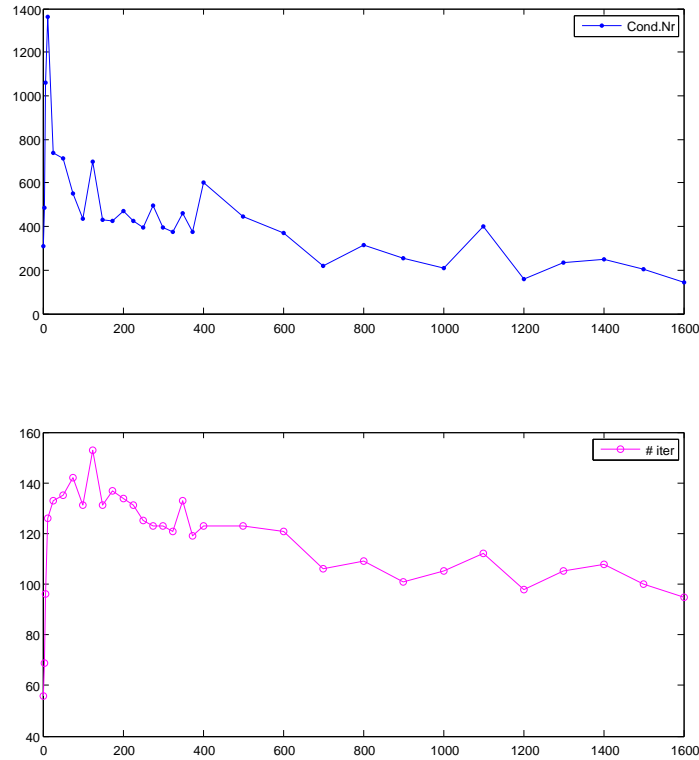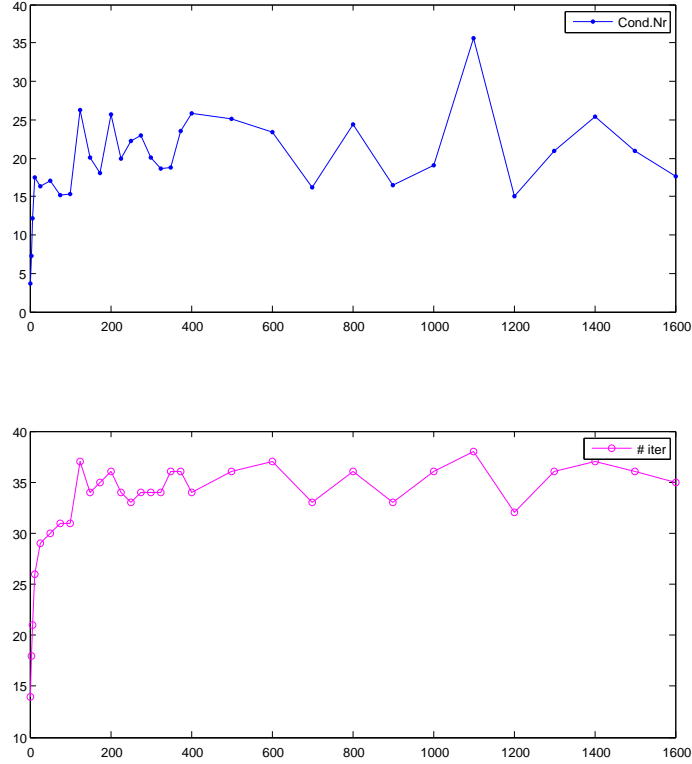
FIGURE 4. Non-preconditioned FETI-type solver for the BEM-based FEM: estimated condition numbers and CG iteration numbers in dependence on the number N of subdomains

N	total time	avg. loc. time	#iter	error	# Lagrange
2	24.503039	2.738385	56	0.000006	709
6	30.922103	0.559905	96	0.000006	2168
25	32.226731	0.077579	133	0.000005	5875
50	30.192864	0.031712	135	0.000006	8962
100	26.638113	0.013545	131	0.000005	13012
150	24.588265	0.008301	131	0.000005	16219
200	23.694787	0.005947	134	0.000005	19056
250	21.909531	0.004601	125	0.000005	21372
300	21.365941	0.003765	123	0.000005	23460
400	21.062826	0.002720	123	0.000005	27324
800	20.233496	0.001295	109	0.000005	39304
1200	20.503277	0.000848	98	0.000005	48813
1600	22.188883	0.000636	95	0.000005	56632

TABLE 1. Some results of the non-preconditioned solver. Columns: number of subdomains, total CPU time for solution, averaged time for solution of local problems, number of iterations, residual error, number of Lagrange multipliers.

FIGURE 5. Preconditioned FETI-type solver for the BEM-based FEM, Dirichlet preconditioner: estimated condition numbers and PCG iteration numbers in dependence of N

N	total time	avg. loc. time	#iter	error	# Lagrange
2	22.9563	2.70074	14	6.45469e-06	709
6	21.7471	0.54795	21	6.39847e-06	2168
25	20.4929	0.0759496	29	4.77774e-06	5875
50	19.1048	0.0310428	30	5.90121e-06	8962
100	17.7017	0.013063	31	4.75217e-06	13012
150	17.5015	0.00799038	34	4.72264e-06	16219
200	17.4147	0.00573496	36	5.14293e-06	19056
250	16.0321	0.00440914	33	4.75428e-06	21372
300	16.1877	0.00360337	34	4.73872e-06	23460
400	16.1319	0.00263458	34	4.73785e-06	27324
800	17.6753	0.00125147	36	4.77933e-06	39304
1200	18.1828	0.000819669	32	4.82913e-06	48813
1600	20.9631	0.000613087	35	4.813e-06	56632

TABLE 2. Some results of the preconditioned solver. Columns: number of subdomains, total CPU time for solution, averaged time for solution of local problems, number of iterations, residual error, number of Lagrange multipliers.

The fast solver presented in this article is based directly on the classical one-level FETI approach. Methods that were developed later, like the dual-primal FETI method (FETI-DP, [5, 18]) or balancing domain decomposition by constraints (BDDC, [3, 15, 16]) could be adapted in a similar fashion, and with the help of the spectral equivalences shown in Section 6, we expect the analysis of these methods to transfer to the case of the BEM-based FEM in a straightforward way.

Acknowledgments

References

[1] D. M. Copeland. Boundary-element-based finite element methods for Helmholtz and Maxwell equations on general polyhedral meshes. *Int. J. Appl. Math. Comput. Sci.*, 5(1):60–73, 2009.

[2] D.M. Copeland, U. Langer, and D. Pusch. From the boundary element method to local Trefftz finite element methods on polyhedral meshes. In M. Bercovier, M. J. Gander, R. Kornhuber, and O. Widlund, editors, *Domain Decomposition Methods in Science and Engineering XVIII*, volume 70 of *Lecture Notes in Computational Science and Engineering*, pages 315–322. Springer-Verlag, Heidelberg, Berlin, 2009.

[3] C. R. Dohrmann. A preconditioner for substructuring based on constrained energy minimization. *SIAM J. Sci. Comput.*, 25(1):246–258, January 2003.

[4] Z. Dostál, D. Horák, and R. Kučera. Total FETI – an easier implementable variant of the FETI method for numerical solution of elliptic PDE. *Commun. Numer. Methods Eng.*, 22(12):1155–1162, 2006.

[5] C. Farhat, M. Lesoinne, P. Le Tallec, K. Pierson, and D. Rixen. FETI-DP: A dual-primal unified FETI method I: A faster alternative to the two-level FETI method. *Internat. J. Numer. Methods Engrg.*, 50:1523–1544, 2001.

[6] C. Farhat, J. Mandel, and F. X. Roux. Optimal convergence properties of the FETI domain decomposition method. *Computer Methods in Applied Mechanics and Engineering*, 115(3–4):365–385, 1994.

[7] C. Farhat and F.-X. Roux. A method of finite element tearing and interconnecting and its parallel solution algorithm. *Int. J. Numer. Meth. Engrg.*, 32:1205–1227, 1991.

[8] C. Hofreither. L_2 error estimates for a nonstandard finite element method on polyhedral meshes. *J. Numer. Math.*, 19(1):27–39, 2011.

[9] C. Hofreither. *A Non-standard Finite Element Method using Boundary Integral Operators*. PhD thesis, Johannes Kepler University, Linz, Austria, December 2012.

[10] C. Hofreither, U. Langer, and C. Pechstein. Analysis of a non-standard finite element method based on boundary integral operators. *Electron. Trans. Numer. Anal.*, 37:413–436, 2010.

[11] C. Hofreither, U. Langer, and C. Pechstein. A non-standard finite element method for convection-diffusion-reaction problems on polyhedral meshes. In Michail D. Todorov and Christo I. Christov, editors, *Application of Mathematics in Technical and Natural Sciences: 3rd International Conference AMiTaNS'11*, volume 1404, pages 397–404. AIP, 2011.

[12] C. Hofreither and C. Pechstein. A rigorous error analysis of coupled FEM-BEM problems with arbitrary many subdomains. In T. Apel and O. Steinbach, editors, *Advanced Finite Element Methods and Applications*, volume 66 of *Lecture Notes in Applied and Computational Mechanics*, pages 109–130. Springer, 2012.

[13] A. Klawonn and O. B. Widlund. FETI and Neumann-Neumann iterative substructuring methods: connections and new results. *Comm. Pure Appl. Math.*, 54(1):57–90, 2001.

[14] U. Langer and O. Steinbach. Boundary element tearing and interconnecting method. *Computing*, 71(3):205–228, 2003.

[15] J. Mandel and C. R. Dohrmann. Convergence of a balancing domain decomposition by constraints and energy minimization. *Numer. Lin. Alg. Appl.*, 10:639–659, 2003.

[16] J. Mandel, C. R. Dohrmann, and R. Tezaur. An algebraic theory for primal and dual substructuring methods by constraints. *Appl. Numer. Math.*, 54:167–193, 2005.

[17] J. Mandel and R. Tezaur. Convergence of a substrucuring method with Lagrange multipliers. *Numer. Math.*, 73:473–487, 1996.

[18] J. Mandel and R. Tezaur. On the convergence of a dual-primal substructuring method. *Numer. Math.*, 88:543–558, 2001.

[19] G. Of and O. Steinbach. The all-floating BETI method: Numerical results. In U. Langer, M. Discacciati, D. E. Keyes, O. B. Widlund, and W. Zulehner, editors, *Domain Decomposition Methods in Science and Engineering XVII*, volume 60 of *Lecture Notes in Computational Science and Engineering*, pages 295–302, Berlin, 2008. Springer-Verlag.

[20] C. Pechstein. *Finite and Boundary Element Tearing and Interconnecting Solvers for Multiscale Problems*, volume 90 of *Lecture Notes in Computational Science and Engineering*. Springer-Verlag, Berlin, Heidelberg, 2013.

[21] C. Pechstein. Shape-explicit constants for some boundary integral operators. *Appl. Anal.*, 92(5):949–974, 2013.

[22] C. Pechstein and R. Scheichl. Analysis of FETI methods for multiscale PDEs. *Numer. Math.*, 111(2):293–333, 2008.

[23] C. Pechstein and R. Scheichl. Analysis of FETI methods for multiscale PDEs. Part II: interface variation. *Numer. Math.*, 118(3):485–529, 2011.

[24] D. Rixen and C. Farhat. A simple and efficient extension of a class of substructure based preconditioners to heterogeneous structural mechanics problems. *International Journal for Numerical Methods in Engineering*, 44(4):489–516, 1999.

[25] D. Rixen, C. Farhat, R. Tezaur, and J. Mandel. Theoretical comparison of the FETI and algebraically partitioned FETI methods, and performance comparisons with a direct sparse solver. *Internat. J. Numer. Methods Engrg.*, 46(4):501–533, 1999.

[26] S. Rjasanow and S. Weißer. Higher order BEM-based FEM on polygonal meshes. *SIAM Journal on Numerical Analysis*, 50(5):2357–2378, 2012.

[27] S. A. Sauter and C. Schwab. *Boundary Element Methods*, volume 39 of *Springer Series in Computational Mathematics*. Springer, Berlin, Heidelberg, 2011.

[28] L. R. Scott and S. Zhang. Finite element interpolation of non-smooth functions satisfying boundary conditions. *Math. Comp.*, 54:483–493, 1990.

[29] O. Steinbach. *Numerical approximation methods for elliptic boundary value problems – Finite and boundary elements*. Springer, New York, 2008.

[30] A. Toselli and O. Widlund. *Domain Decoposition Methods – Algorithms and Theory*, volume 34 of *Springer Series in Computational Mathematics*. Springer-Verlag, Berlin, Heidelberg, 2005.

[31] S. Weißer. Residual error estimate for BEM-based FEM on polygonal meshes. *Numerische Mathematik*, 118(4):765–788, 2011.

[32] S. Weißer. *Finite Element Methods with local Trefftz trial functions*. PhD thesis, Universität des Saarlandes, Saarbrücken, Germany, 2012.

Latest Reports in this series

2009 - 2011

[..]

2012

[..]

2013